# Numerical Analysis of the Injection Moulding Behaviour of Short Fibre Filled PET

A. A. ERHERIENE and J. M. HODGKINSON

Centre for Composite Materials, Imperial College of Science, Technology and Medicine, Prince Consort Road, London SW7 2BY

## Abstract

The behaviour of short fibre filled polyethylene terephthalate melt during the filling of an irregularly shaped thin cavity is analysed numerically. The flow is assumed to be a Hele-Shaw and a coupled solution procedure is described for the stream function and the energy equations. The solution of the governing flow equation as the fluid domain deforms and enlarges is described by the use of numerically generated meshes that conform to the fluid boundaries at every time step. The temperature field during filling is shown to be three-dimensional with convection dominating the planar flow, and diffusion across the thin gapwith. The flow front is considered as fountain flow and suggestions are put forward as to how to tackle the heat transfer problem in this region. Motion of the fibres is described using the Dinh-Armstrong model which was developed for semi-concentrated fibre suspensions.

## 1. Introduction

Unfilled PET resins exhibit excellent mechanical, electrical and chemical properties but suffer from poor processability, low distortion temperature and poor impact resistance. Perhaps the most severe defficiency of PET is its poor processability which is due to its slow crystallisation rate.

Glass fibre reinforced PET resins overcome two of the above deficiencies. The heat deflection temperature rises spectacularly, while impact properties are also significantly improved. Processability still remains a problem, however, as the need for high mould temperatures leads to relatively long cycle times.

The problem involving flow in an injection mould where filling is difficult does require inclusion of heat transfer cooling of the polymer. If the moulding conditions, such as thin walls, long flow sections, or extremely viscous moulding materials threaten short shot occurrence, then temperature changes must be included in the problem scope. It would be useful to know if a mould of a certain cavity geometry, with a specific material of known thermodynamic and rheometric properties, will result

in a successful fill or result in a short shot.

In many injection moulding processes short fibre filled polymeric suspensions are often used. Whenever such a material is formed, the flow changes the orientation of the fibres. This fibre orientation pattern is the dominant feature of a short fibre composite. The composite is stiffer and stronger in the direction of greatest orientation, and weaker and more compliant in the direction of least orientation. Theories exist which can predict the mechanical properties of the composite once the fibre orientation is known(1,2,3,4).

In this investigation, we have used a computational code (5) to analyse the flow of short fibre filled PET melt in an injection moulding process.

## 2. Theoretical considerations

Basic rheological equations of state

Many equations of state have been developed over a period of time to help in the understanding of general flow behaviour of fluids through thin cavities as encountered in injection moulding process.

We can quite easily combine equations (6) corresponding to shearing in different planes, in a single equation relating the stresses $P_{ik}$ which correspond to a rate- of- strain tensor $e_{ik}$ :

$$P_{ik} + \lambda_1 \frac{dP_{ik}}{dt} = 2\eta_o\left(e_{ik} + \lambda_2 \frac{de_{ik}}{dt}\right) \qquad [1]$$

$\eta_o$ = viscosity, $\lambda_1$ = relaxation time, $\lambda_2$ = retardation time

If the material is assumed incompressible , any isotropic pressure can be superposed without affecting the deformation, so that the full stress tensor can be written as :

$$P_{IK} = P_{ik} - \Pi\delta_{ik} \qquad [2]$$

where $\Pi$ is arbitrary

In these equations the components $e_{ik}$ of rate of strain are defined in the usual way, in terms of the velocity components $v_i$ in the three fixed orthogonal cartesian coordinate directions $Ox_i$, by the formula :

$$e_{ik} = \frac{1}{2}\left[\frac{\partial v_k}{\partial x_i} + \frac{\partial v_i}{\partial x_k}\right] \qquad [3]$$

The stresses are also defined in the usual way with reference to the orthogonal cartesian coordinate system (with the sign convention that a positive $P_{11}$ denotes a tension, a negative $P_{11}$ denotes pressure ). In simple shearing :

$$P_{12} = P_{21} = \tau \text{ and } e_{12} = e_{21} = \frac{\gamma}{2}$$

are the only non-vanishing components of stress and rate of strain, so that above equations [1] and [2] reduce to :

$$\tau + \lambda_1\dot{\tau} = \eta_0(\gamma + \lambda_2\dot{\gamma}) \qquad [4]$$

$$\lambda_1 > \lambda_2 > 0$$

The derivative of the quantities in the equations of state should be defined in such a way as to have physical significance. (a) The derivative should measure a rate of change following a particle of the fluid. (b) It should measure an intrinsic property of a typical material element which at time t is at $(x_1, x_2, x_3)$ when applied to a scalar quantity like pressure or temperature. (c) It should account for the rotation of the material by measuring vorticity components, as well as for the translation of the material by measuring velocity components. A suitable definition for any material derivative of any second order tensor, such as $e_{ik}$ and $P_{ik}$ is given by (7)

$$\frac{De_{ik}}{Dt} = \frac{\partial e_{ik}}{\partial t} + \sum_j v_j \frac{\partial e_{ik}}{\partial x_j} + \sum_j w_{ij} e_{jk} + \sum_j w_{kj} e_{ij} \qquad [5]$$

$$\frac{DP_{ik}}{Dt} = \frac{\partial P_{ik}}{\partial t} + \sum_j v_j \frac{\partial P_{ik}}{\partial x_j} + \sum_j w_{ij} P_{jk} + \sum_j w_{kj} P_{ij} \qquad [6]$$

$$w_{ik} = \frac{1}{2}\left[\frac{\partial v_i}{\partial x_k} - \frac{\partial v_k}{\partial x_i}\right] = \text{vorticity}$$

It is necessary to simplify equations [5] and [6] to make them usable. Several models have been developed from these equations, here we consider those of Oldroyd (7) and Zaremba (8)

Oldroyd A

$$\frac{\partial P_{ij}}{\partial t} + \frac{\partial v_m P_{mj}}{\partial x_i} + \frac{\partial v_m P_{mi}}{\partial x_j} = 2Ge_{ij} - \frac{1}{\lambda} P_{ij} \qquad [7]$$

$$e_{ij} = \frac{1}{2}\left[\frac{\partial v_i}{\partial x_j} + \frac{\partial v_j}{\partial x_i}\right] \text{ the deformation tensor}$$

$\lambda$ is associated with the relaxation time

Oldroyd B

$$\frac{\partial P_{ij}}{\partial t} - \frac{\partial v_m P_{mj}}{\partial x_i} - \frac{\partial v_m P_{mi}}{\partial x_j} = 2Ge_{ij} - \frac{1}{\lambda} P_{ij} \qquad [8]$$

In both cases G is associated with the modulus of material

Either of the Oldroyd equations can be used to solve flow problems in thin cavities at steady state. For example, define a problem such that:

$$v_1 = \dot{\gamma} x_2 \ , \ v_2 = v_3 = 0$$

When Oldroyd A is applied to this problem the following solutions are obtained:

$$P_{11} = 0$$

$$P_{22} = -2\lambda P_{12} \frac{\partial v_1}{\partial x_2} \ , \quad P_{33} = 0 \ , \ P_{12} = P_{21} = \lambda G \frac{\partial v_1}{\partial x_2}$$

$$P_{13} = P_{31} = P_{23} = P_{32} = 0$$

$$N_1 = P_{11} - P_{22} = 2\lambda P_{12} \frac{\partial v_1}{\partial x_2}$$

$$N_2 = P_{22} - P_{33} = -2\lambda P_{12} \frac{\partial v_1}{\partial x_2}$$

$P_{ij}$ $(i = j)$ normal stress

$(i \neq j)$ shear stress

$N_1$ = first normal stress difference, $N_2$ = second normal stress difference

So that using the Oldroyd A model we are able to calculate normal stress, shear stress, and normal stress differences.

Zaremba model

$$\frac{\partial P_{ij}}{\partial t} + w_{im} P_{mj} + w_{jm} P_{im} = 2Ge_{ij} - \frac{1}{\lambda} P_{ij} \qquad [9]$$

$$w_{ij} = \frac{1}{2}\left[\frac{\partial v_i}{\partial x_j} - \frac{\partial v_j}{\partial x_i}\right]$$

This model was subsequently restated by Dewitt(8).

More recently, Leonov developed what is now known as the Leonov model (9). The Leonov model is based upon the thermodynamics of irreversible processes, and is capable of describing polymeric behaviour under arbitrary elastic deformation. The model has been found to correctly describe steady shear flow, the transition from rest state to steady-state shear flow, stress relaxation following cessation of steady shear flow and the superposition of small-amplitude oscillatory motion

upon steady shear flow of a polymeric solution. The Leonov model can be represented as :

$$P_{ij} = 2\sum_{k=1} \mu_k C_{ij,k} + 2\mu s\dot{\gamma}\theta_k$$

where

$C_{ij,k}$ = components of elastic strain tensor in the $k^{th}$ relaxation mode

$\mu_k$ = shear modulus in the $k^{th}$ relaxation mode

$\mu$ = shear modulus

s = dimensionless rheological parameter ($0<s<1$)

$\theta_k$ = relaxation time in the $k^{th}$ relaxation mode.

The Leonov model has been used by Isayev et al (10) to relate stress and flow fields in an injection moulding process to demonstrate the usefulness of Leonov's model in solving flow problems.

Hele - Shaw flow

Classical Hele-Shaw flow in a thin cavity of arbitrary shape for an inelastic non-Newtonian fluid under non-isothermal conditions, is governed by (11):

$$0 = \frac{\partial}{\partial z}\left(\eta \frac{\partial u}{\partial z}\right) - \frac{\partial p}{\partial x},$$

$$0 = \frac{\partial}{\partial z}\left(\eta \frac{\partial v}{\partial z}\right) - \frac{\partial p}{\partial y}$$

$$\frac{\partial}{\partial x}(b\bar{u}) + \frac{\partial}{\partial y}(b\bar{v}) = 0$$

$$\rho C_p\left(\frac{\partial T}{\partial t} + u\frac{\partial T}{\partial x} + v\frac{\partial T}{\partial y}\right) = k\frac{\partial^2 T}{\partial z^2} + \eta\dot{\gamma}^2$$

where b is the half gapwidth, the bar denotes an average over z, the gapwise coordinate, and the shear viscosity is taken to be of the form:

$$\eta = \eta(\dot{\gamma}, T)$$

where

$$\dot{\gamma} = \left[\left(\frac{\partial u}{\partial z}\right)^2 + \left(\frac{\partial v}{\partial z}\right)^2\right]^{\frac{1}{2}}$$

These Hele-Shaw model equations are based on several rather crude

approximations: (i) the neglect of normal-stress and memory effects associated with fluid elasticity; (ii) the neglect of the "fountain" flow region in the vicinity of the advancing melt front, together with its effect upon the temperature field; (iii) the neglect of thermal convection in the gap-wise direction. However earlier one-dimensional and two-dimensional flow simulations have invoked all of the above approximations and still provided results in reasonable agreement with experimental pressure measurements (11). The computer code developed by Guceri et al (5) used for this investigation is based on the Hele-Shaw flow model.

Short fibre orientation

The characterisation of short fibre orientation in a short fibre suspension is a major concern in current polymer processing research. Several studies have characterised the orientation state in fibre suspension systems. Jeffery's (12) early work on the motion of an ellipsoid in a viscous Newtonian fluid has been used by Givler et al (13) to develop a computer code to predict the orientation angle in dilute suspensions in confined geometries. Folger and Tucker (14) proposed a phenomenological model which incorporates the effects of the interaction among rigid fibres. In their paper, they used an orientation distribution function to describe the fibre orientation for non-dilute fibre suspensions. Dinh and Armstrong (15) developed a rheological model for semi-concentrated suspensions. In this model a constitutive equation which requires the calculation of the fourth-order moments of the distribution function is proposed to calculate the rheological properties.
All of the proposed models for fibre suspensions require some form of description of the fibre orientation. The simplest case is the use of a scalar which is usually the angle between the fibre axis and one of the reference axes. For 3-D cases $\theta$ and $\phi$ must be used to specify the orientation angle in spherical coordinates (14). At a given point and time, the orientation distribution function for fibres provides a complete description of the orientation state (16). The solution of the orientation distribution function has aroused much interest. The governing equation is a linear partial differential equation (PDE) and is also known as the Fokker-Planck equation. No analytical solution is available when particles in suspension are small enough for "Brownian" effects to be considered. Although the orientation distribution function contains the complete description, it is not always necessary to make use of this function (17).
In this investigation, we employ the Dinh-Armstrong model for a semi concentrated fibre suspension. We also show Guceri's (5) illustration of how the solution of the distribution function is obtained in terms of flow kinematics.

Dinh-Armstrong model(14)

$$\sigma_{ij} = \mu \frac{\prod l^3 n}{6 \ln(Q)} \int u_{k,l} P_k P_l P_i P_j \psi(P, t) dP \qquad [10]$$

$\sigma_{ij}$ stress tensor generated in the homogeneous stress fields due to the presence of of particles.

n number density of suspension

l fibre diameter

$P_i$ $i^{th}$ component of the unit vector denoting the fibre orientation

$\psi(P, t)$ distribution function for the fibre orientation

H average distance from a given fibre to its nearest neighbour
= $(nl)^{-1/2}$ for aligned systems
= $(nl^2)$ for random systems

$\mu$ absolute viscosity of the fluid

$u_{k,l} = \partial u_k / \partial x_l$ components of the velocity gradient tensor

Equation [10] can be rewritten as

$$\sigma_{ij} = \mu \frac{\prod l^3 n}{6 \ln(Q)} u_{k,l} S_{ijkl} \qquad [11]$$

where

$S_{ijkl}$ is the fourth moment of the distribution function and is defined as the fourth-order orientation tensor.
The equation of motion for the fibres can be expressed in the form of Jeffery's equation with infinite aspect ratio (15):

$$\dot{P} = u_{i,q} P_q - u_{k,q} P_q P_k P_i \qquad [12]$$

Equation [12] is already built in equation [11] and the coefficient of the integral in equation [10] is determined by using structural analysis of semi concentrated suspensions (18).

Solution for the distribution function

Given the initial condition of random fibres

for two-dimensions

$$\psi(\theta, t = 0) = \frac{1}{\prod} \qquad [13]$$

for three-dimensions

$$\psi(\theta, \phi, t = 0) = \frac{1}{4\prod} \qquad [14]$$

$$\Psi_\theta(P,t) = \frac{1}{\Pi}\left(\Delta.\Delta^{+} : \bar{P}\bar{P}\right)^{-1} \qquad [15]$$

$$\Psi(\bar{P},t) = \frac{1}{4\Pi}\left(\Delta.\Delta^{+} : \bar{P}\bar{P}\right)^{\frac{3}{2}} \qquad [16]$$

where

$\Delta$ is the deformation tensor and + implies its transpose and is defined as

$$\Delta_{ij} = \frac{\partial x_i'}{\partial x_j} \qquad [17]$$

in which $x'_i$ is the position vector at t = 0 and $x_j$ is the position vector at time t. The solution to equation [15] can be explicitly written as (5)

$$\Psi_\theta(\theta,t) = \frac{1}{\Pi}\left[(\Delta_{11}^2 + \Delta_{21}^2)P_1^2 + (\Delta_{11}\Delta_{12} + \Delta_{21}\Delta_{22})2P_1P_2 + (\Delta_{12}^2 + \Delta_{22}^2)P_2^2\right]^{-1} \qquad [18]$$

where

$$P = \begin{pmatrix} P_1 \\ P_2 \end{pmatrix} = \begin{pmatrix} \cos\theta \\ \sin\theta \end{pmatrix}$$

The three dimensional solution of the distribution function can be explicitly written from equation [16] as (5)

$$\begin{aligned}\Psi(\theta,\phi,t) = \frac{1}{4\Pi}\Big[&(\Delta_{11}^2 + \Delta_{21}^2 + \Delta_{31}^2) + (\Delta_{11}\Delta_{12} + \Delta_{21}\Delta_{22} + \Delta_{31}\Delta_{32})2P_1P_2 \\ &+ (\Delta_{11}\Delta_{13} + \Delta_{21}\Delta_{23} + \Delta_{31}\Delta_{33})2P_1P_3 \\ &+ (\Delta_{12}^2 + \Delta_{22}^2 + \Delta_{32}^2)P_2^2 \\ &+ (\Delta_{12}\Delta_{13} + \Delta_{22}\Delta_{23} + \Delta_{32}\Delta_{33})2P_2P_3 \\ &+ (\Delta_{13}^2 + \Delta_{23}^2 + \Delta_{33}^2)P_3^2\Big]^{\frac{3}{2}}\end{aligned} \qquad [19]$$

where:

$$P = \begin{pmatrix} P_1 \\ P_2 \\ P_3 \end{pmatrix} = \begin{pmatrix} \sin\theta\cos\phi \\ \sin\theta\sin\phi \\ \cos\theta \end{pmatrix}$$

## 3 Numerical solution procedure

The ability to predict the flow characteristics and fibre orientation during injection moulding is of significant interest today. A computer code developed by Guceri et al (5) was used for this investigation. The computer code uses a viscosity model to describe the flow behaviour of

the fluid and it uses the Dinh-Armstrong model to predict the fibre orientation at every point in time as the fluid fills the mould. The computer code uses finite difference technique that allows for continuous generation of meshes that are enlarged and deformed to follow the injected fluid and fibres as the mould is being filled. The governing flow equations, the energy equation, the constitutive equation and the short fibre orientation are solved simultaneously (19).

Viscosity model

Although there are many viscosity models we have considered two which show viscosity to be both temperature and shear rate dependent.

(i) Carreau/Arrhenius model

This model can be expressed as (19):

$$\eta_v = \eta(\dot{\gamma}) \mathrm{Exp}\left[-\frac{(T - T_o) A_n}{T_o}\right] \qquad [20]$$

$$\eta(\dot{\gamma}) = \eta_\infty + (\eta_o + \eta_\infty)\left[1 + (\lambda\dot{\gamma})^2\right]^{\frac{n-1}{2}} \qquad [21]$$

where

$T$ operating temperature

$T_o$ reference temperature

$A_n$ Arrhenius constant ( an empirical constant obtained from experimental ) ( observations over a range of temperatures and shear rates)

$\eta_v$ kinematic viscosity ( operating viscosity )

$\eta_o$ zero shear rate viscosity

$\eta_\infty$ viscosity at infinite shear rate

$\lambda$ time constant (associated with relaxation time)

$n$ dimensionless power law index

Although the Carreau model describes polymer melt viscosity fairly well it has one drawback. It is impossible to measure viscosity at infinite shear rate. It is customary to regard the infinite shear rate viscosity as zero. The Carreau model does not represent fibre filled polymer materials very well.

Cross/Arrhenius model (modified)

The modified Cross/Arrhenius equation is(20)

$$\eta_v = \frac{\eta_o(T)}{1 + (\eta_o \dot{\gamma}\alpha)^{1-n}}$$

where

$\alpha = \frac{1}{\sigma}$ , $\sigma$ stands for the shear stress level at which $\eta_v$ is in transition between the Newtonian limit $\eta_o$ and the power law asymptote corresponding to large $\dot{\gamma}$.

$$\eta_o(T) = B_n Exp(\frac{T_b}{T})$$

$B_n$ empirical constant

$T_b$ a measure of the temperature sensitivity of $\eta_o$

T operating temperature

For large shear rates:

$$\eta_v \sim \eta_o^n(\sigma)^{1-n}\gamma^{n-1} = B_n^n(\sigma)^{1-n} Exp(\frac{nT_b}{T})\gamma^{n-1}$$

This model is good for the description of fibre filled thermoplastic materials and rubber compounds. It has the additional advantage of reducing the temperature sensitivity by the factor 'n' in the power-law region.

## 4 PET sample results

Non-isothermal filling of the mould geometry

Non-isothermal flow is simulated for the mould cavity shown in Fig.1. PET is the injected fluid. The mould shape is approximately 19.6 cm long,2 cm wide and has gapwidth of 0.32 cm. A constant inlet velocity of 40 $cms^{-1}$ is used. Inlet temperature used is 290°C. The mould walls are held at constant temperature of 85°C. Cross/Arrhenius viscosity model is used. The Cross coefficients of viscosity for PET at 290°C are taken as:

$\eta_o = 1.81 * 10^2 Nm^{-2}s$

$\alpha = 7.19 * 10^{-2} kN^{-1}m^2$

$\gamma = 3.06 * 10^{-2} s^{-1}$

$n = 0.5$

A sample of the meshes generated during the filling is shown in Fig. 2. The temperature dependence is modelled using T = 290°C, $T_b = 0.024°C^{-1}$. $B_n$ is calculated to be 0.41. At the beginning of injection, a 5 x 15 x 10 mesh is used and this is continuously enlarged to a final mesh size of 70 x 15 x 10 at the instant of complete fill. The time step used is 0.0001 s The pressure distribution at the completion of the filling stage is shown in Fig. 3. At the instance of mould fill, the pressure in the inlet gate is predicted to be 1738. $1kP_a$.

Temperature profile

The three-dimensional temperature solution is displayed (Fig. 4) as a set of contour plots in the x-y plane for three different layers in the mould gapwidth: (a) the surface layer (i.e at z = 0.01111 cm); (b) the second layer (i.e at z = 0.0222 cm), (c) the fifth layer (i.e at z = 0.0555cm). The temperature profile when the mould is completely filled is shown in Fig. 5. The large temperature gradients near the mould walls are clearly seen. The temperature at the free surface is higher than its neighbouring points. This is probably due to fountain flow effect where fluid is

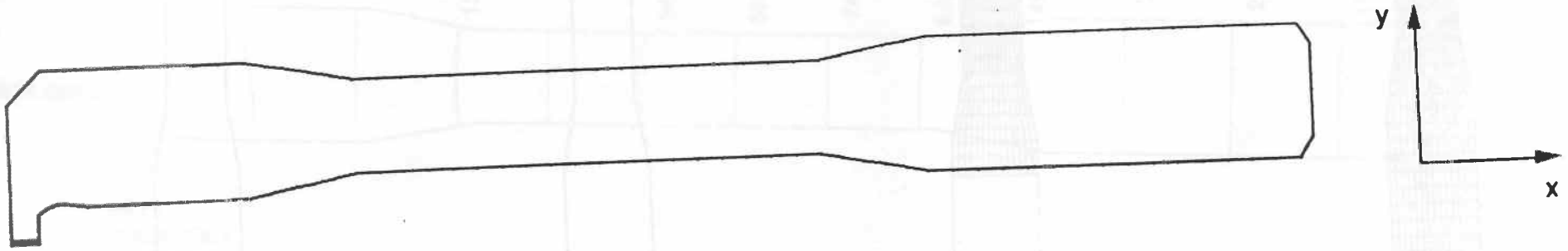


FIG. 1. Problem initialization: the mould shape is specified by user-input nodes along the boundary. An initial fluid domain is assumed in the inlet gate and an initial mesh is generated here.

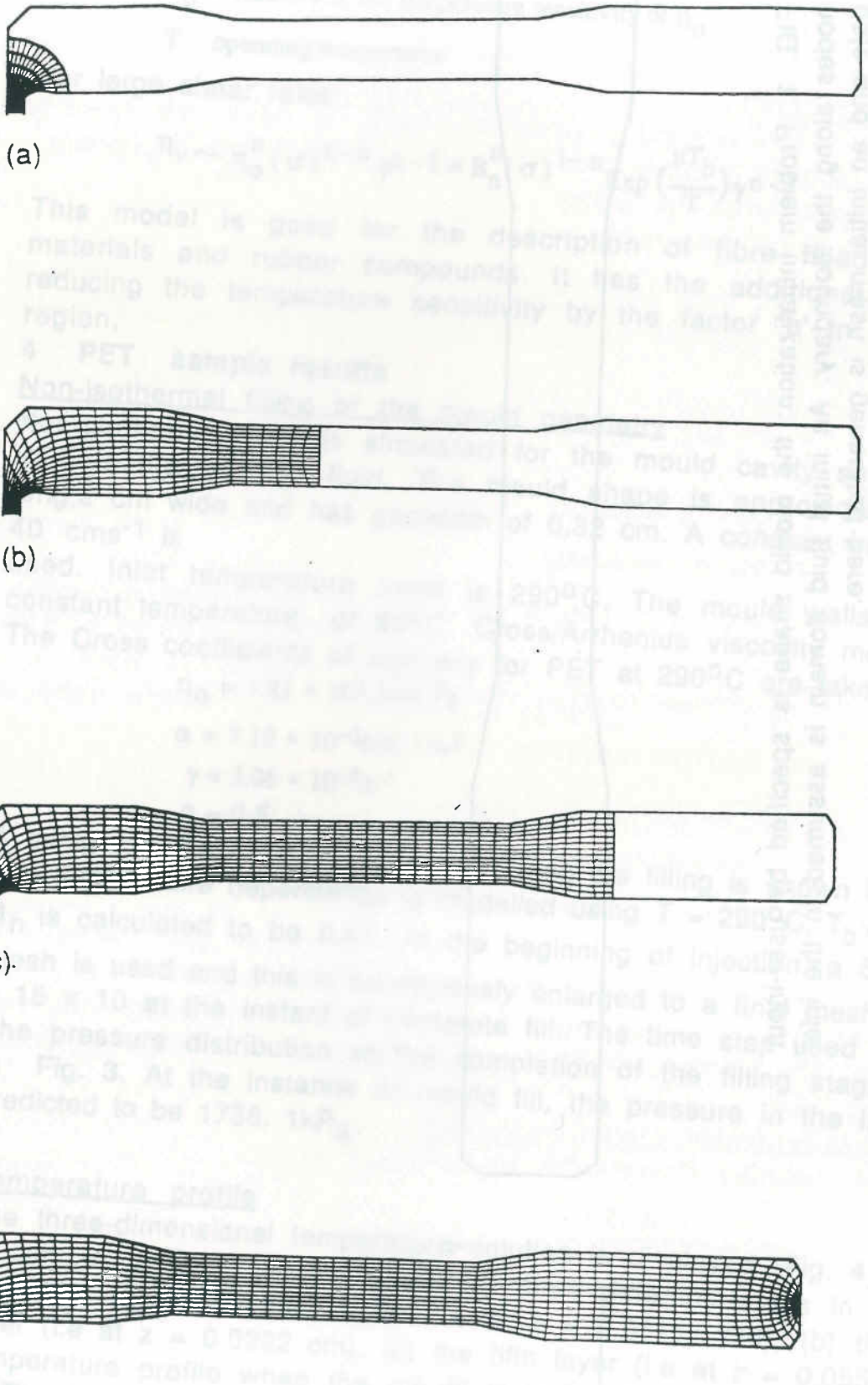


FIG. 2. Irregular mould geometry: the numerically generated meshes over the flow domain at selected times during the filling simulation.

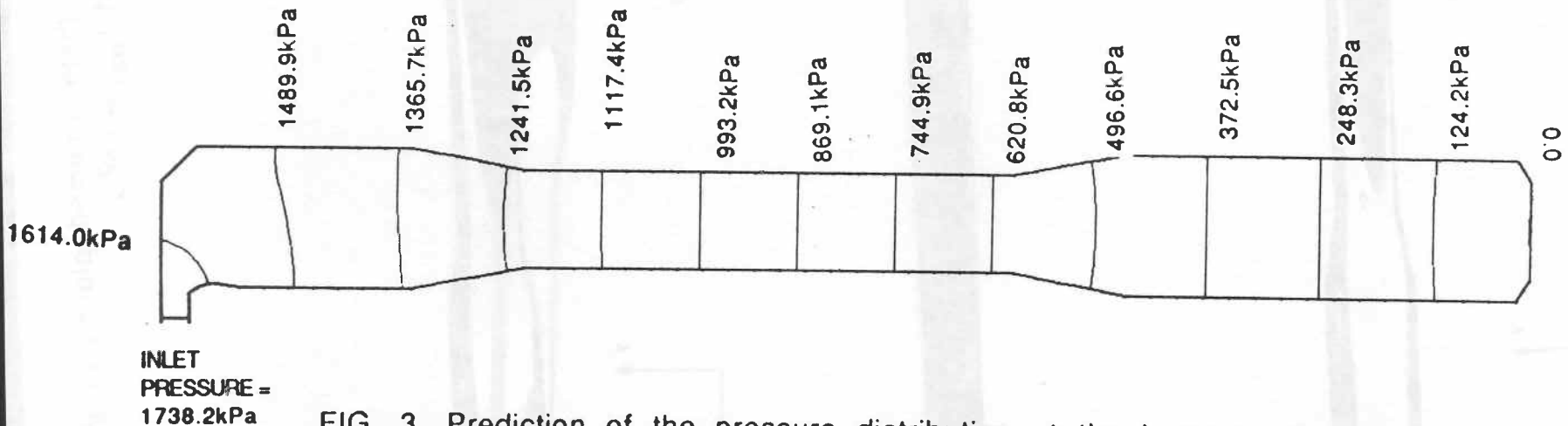


FIG. 3. Prediction of the pressure distribution at the instance of mould fill. Injection pressure at inlet is 1738.2 kPa,each contour corresponds to a step of 124.2 kPa.

FIG. 4. The isotherms at three selected planes in the thickness (gap) direction, $T_{inlet} = 290^{o}C$ and $T_{wall} = 85^{o}C$.

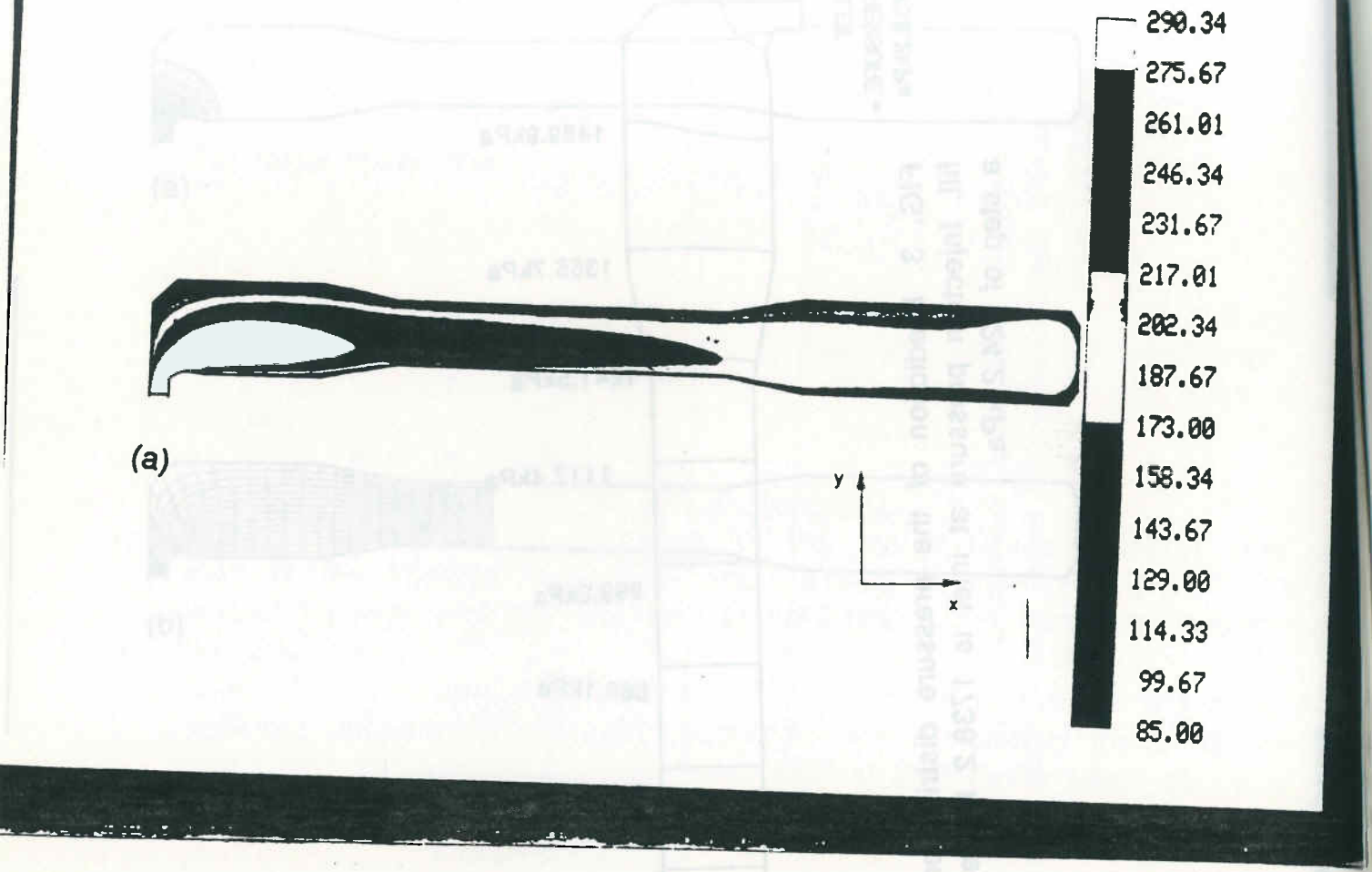


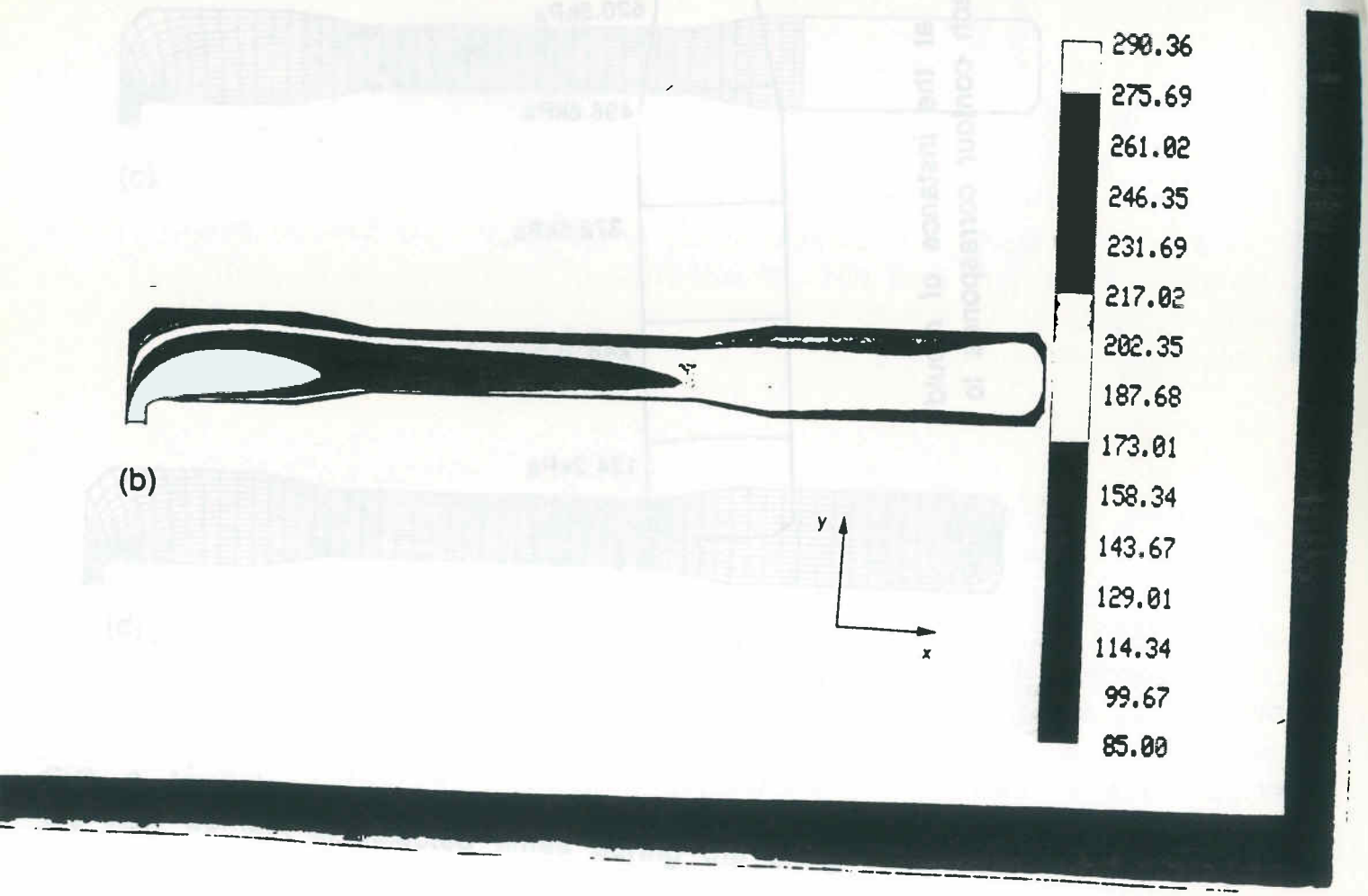

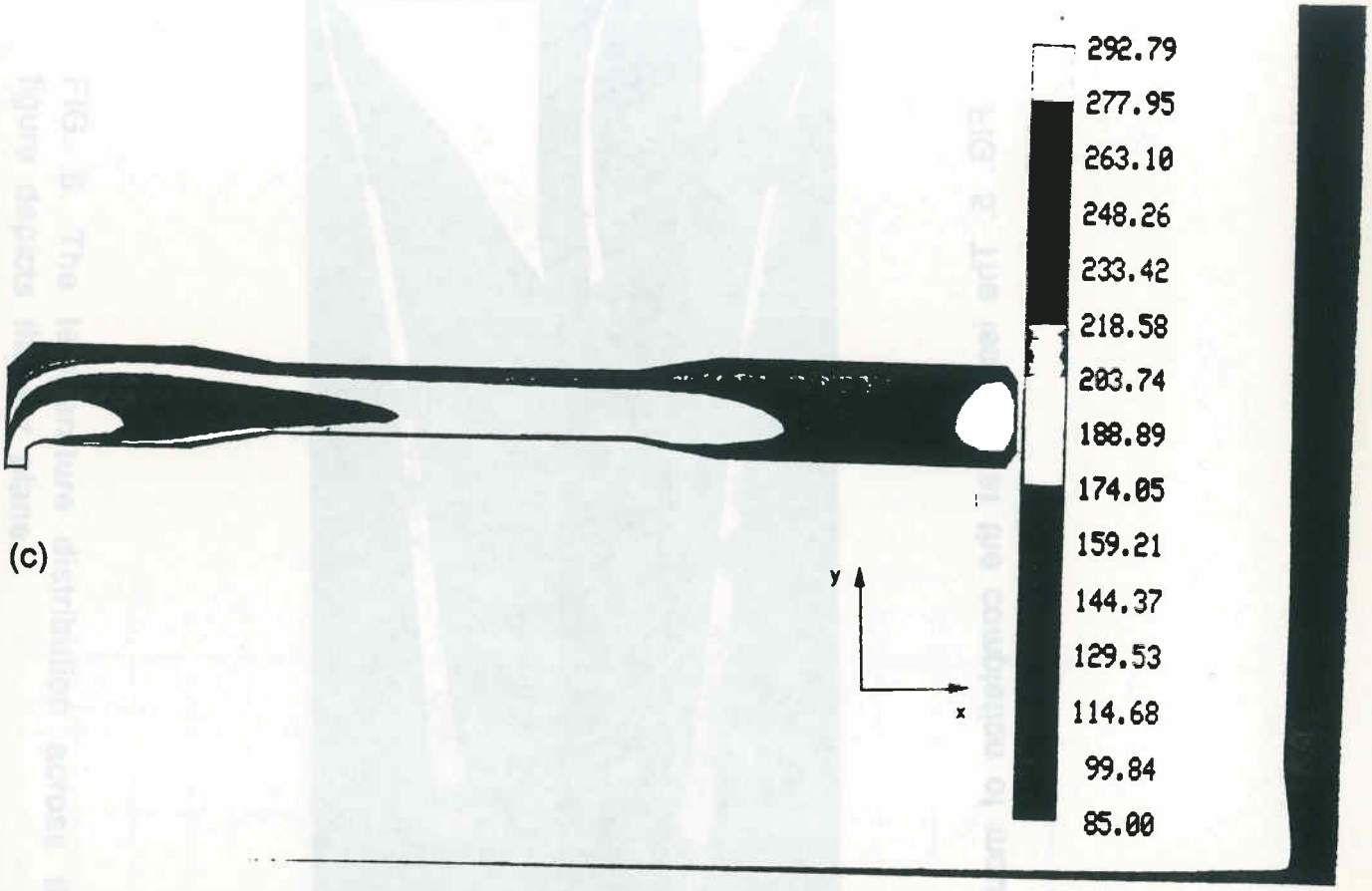
292.79
277.95
263.10
248.26
233.42
218.58
203.74
188.89
174.05
159.21
144.37
129.53
114.68
99.84
85.00
y
x

(c)

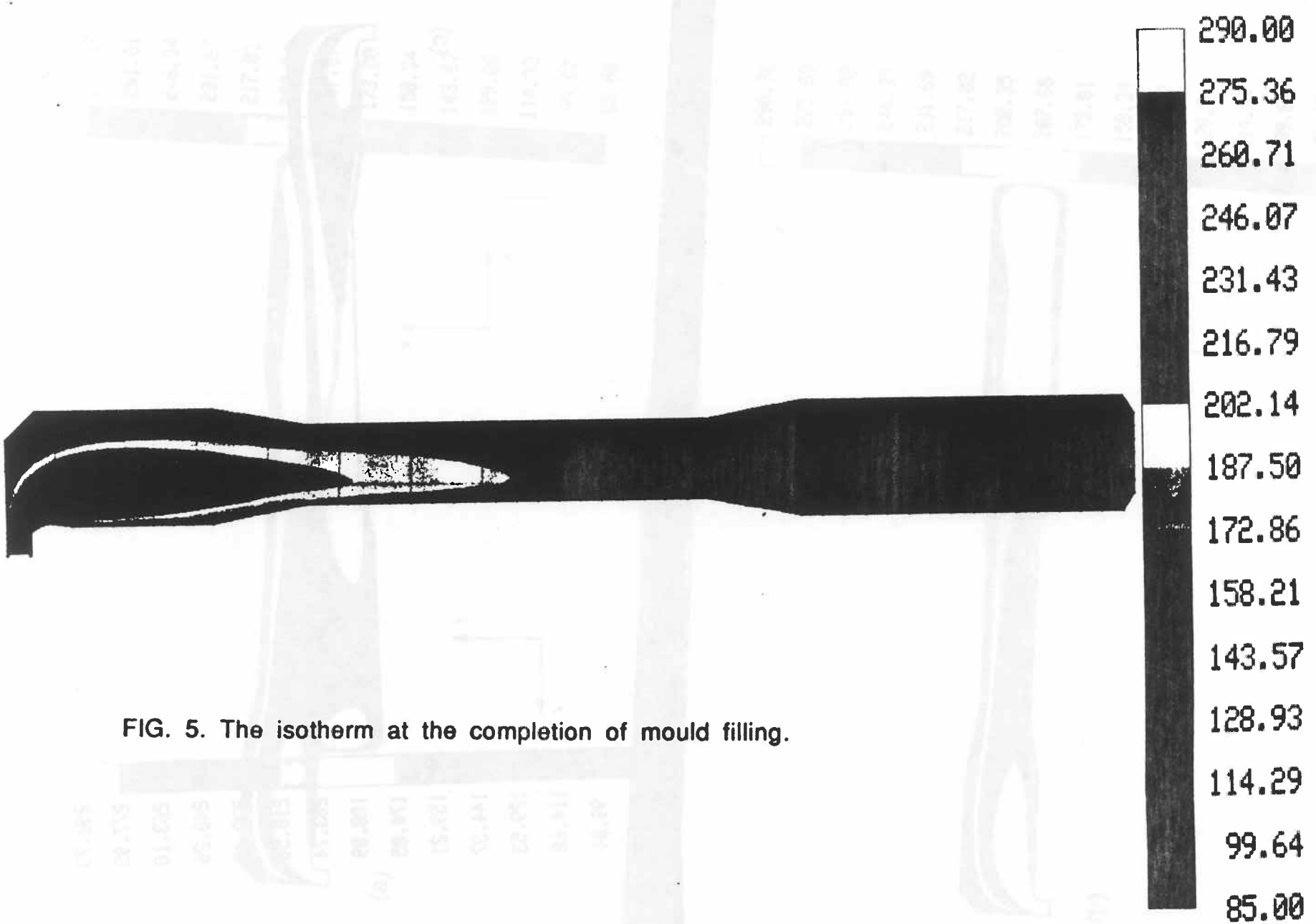


FIG. 5. The isotherm at the completion of mould filling.

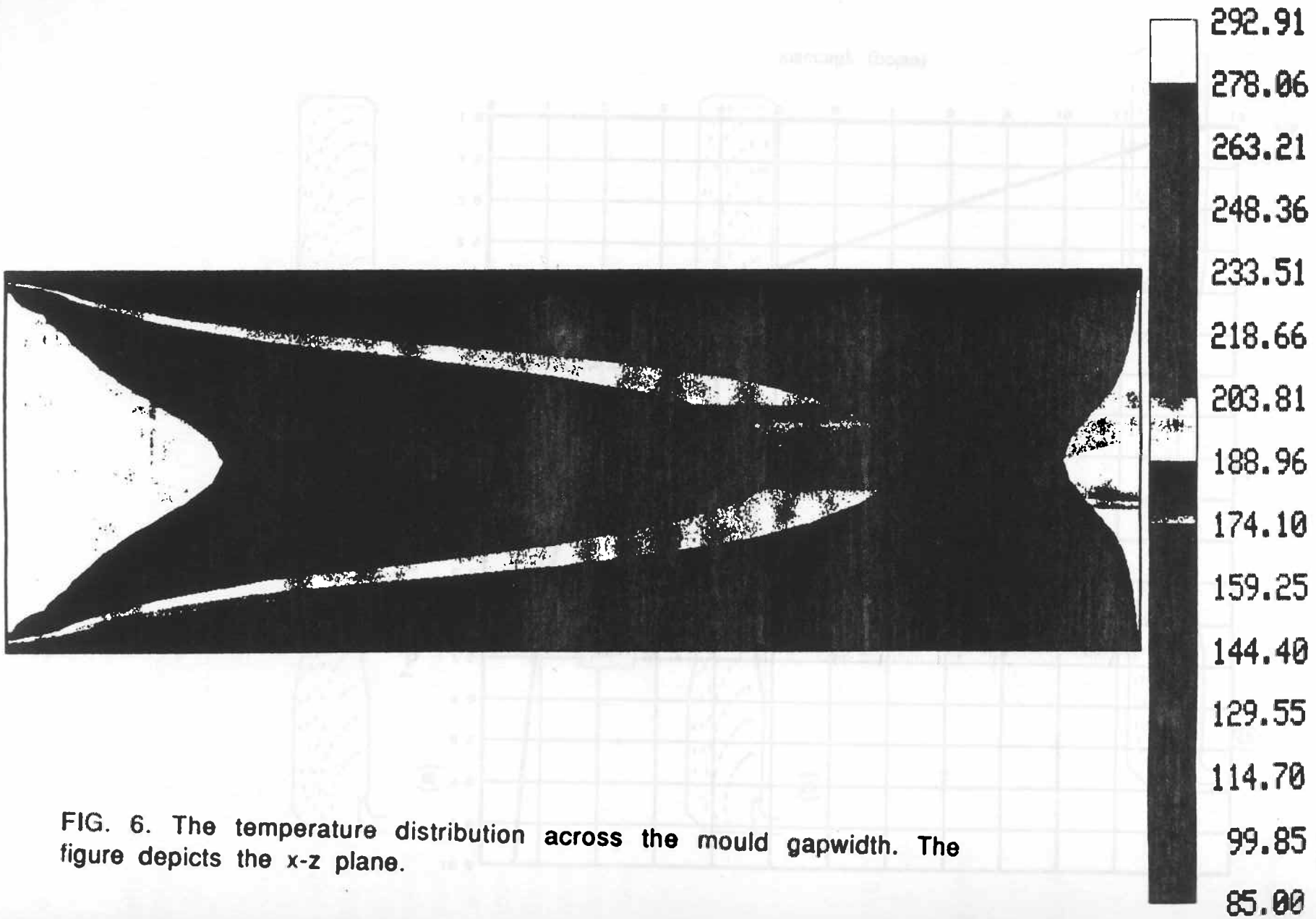


FIG. 6. The temperature distribution across the mould gapwidth. The figure depicts the x-z plane.

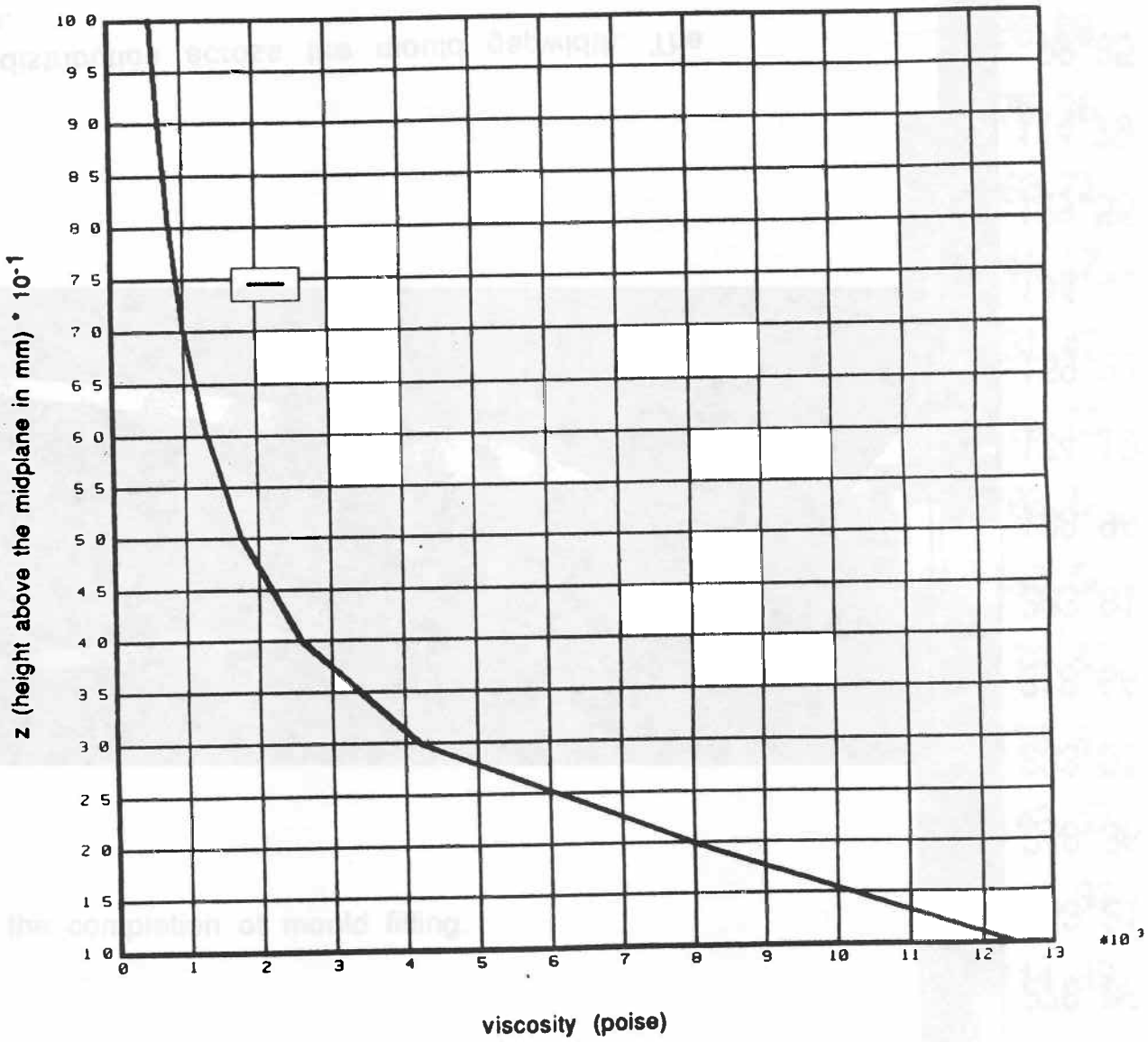


FIG. 7. The gapwise distribution of the viscosity during the filling of the mould.

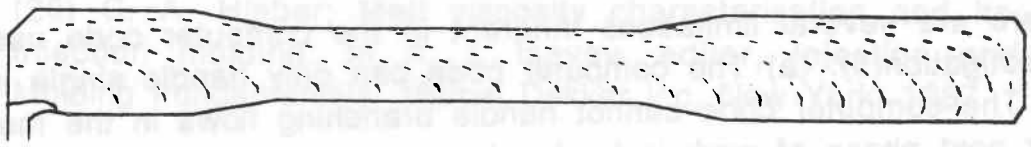

(a)

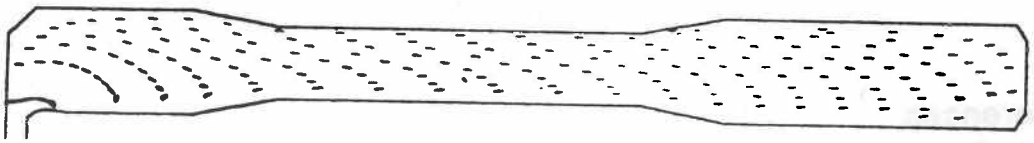

(b)

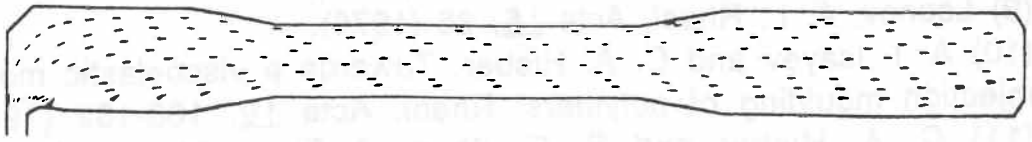

(c)

FIG. 8. The predicted fibre orientations at fill for three selected planes in the gap direction.

convected up from the warmer mould mid-plane.
Temperature distribution through the mould gapwidth is shown in Fig.6 The temperature is seen to exceed the inlet temperature. This is probably due to shear heating during the flow. The viscosity distribution across the gapwidth is depicted in fig.7. There is large variation due to the strong temperature and shear rate dependence of the fluid.

Fibre orientation prediction

The prediction of fibre orientation is shown in Fig. 8. Three different layers in the mould gapwidth are chosen to display the fibre orientations in the x-y plane: (a) at z = 0.01111cm, (b) at z = 0.02222cm, (c) at z = 0.05555cm.

## 5. Further work

There are several limitations inherent in the computer code used for this investigation(5). (a) The computer code can only handle single inlet gates. (b) The computer code cannot handle branching flows in the mould cavity. Our next phase of work is to develop a computer code that can overcome the above limitations. It is our intention to regard the flow as fountain flow and can then use the Galerkin finite element method to calculate the steady state free surface flow for an incompressible non-Newtonian liquid under non-isothermal conditions. The Navier-Stokes equations (where both inertia and gravity are included) will be solved. We propose to solve for velocities, pressure, and free surface location simultaneously by a full Newton iteration. Fibre orientation will be solved using the equations currently under development.

References

(1) J. C. Halpin and J. L. Kardos, Polym. Eng. Sci. , 18, 496(1978).
(2) J. C. Halpin and N. J. Pagauo, J. Compos. Mat., 3, 720(1969).
(3) J. C. Halpin, K. Jerine, and J. M. Whitney, J. Compos.. Mat. 5, 36 (1971).
(4) R. B. Pipes, R. L. McCullough, and D. G. Taggart, Polym. Compos. 3, 34 (1982).
(5) S. I. Guceri, Private Communications, Center For Composite Materials, University of Delaware, Newark, Delaware 19716, U. S. A.
(6) J. G. Oldroyd, Proc. Royal Soc. London, A200, 523 (1950).
(7) J. G. Oldroyd, General Lecture delivered at the Third International Congress on Rheology; Bad Oeynhausen, September 1958.
(8) Dewitt, J., J. Appl. Phys. 26 889 (1955).
(9) Leonov, A. I., Rheol. Acta 15, 85 (1976).
(10) A. I. Isayev and C. A. Hieber; Towards a viscoelastic modelling of the injection moulding of polymers: Rheol. Acta 19, 168-182 (1980).
(11) C. A. Hieber and S. F. Shen; A Finite Element/Finite Difference Simulation of the Injection Molding Filling Process: J. Non-Newtonian Fluid Mech. 7, 1 (1980).
(12) G. B. Jeffery, Proc. Royal Soc., A102, 161 (1922).

(13) R. C. Givler, M. J. Crochet and R. B. Pipes, J. Compos. Mat., 17, 330 (1983).
(14) F. P. Folgar and C. L. Tucker, J. Reinf. Plast. Compos., 3, 98 (1984).
(15) S. M. Dinh and R. C. Armstrong, J. Rheol., 28, 207 (1984).
(16) W. C. Jackson, S. G. Advani and C. L. Tucker, J. Compos. Mat., 20, 539 (1986).
(17) M. C. Altan, S. G. Advani, S. I. Guceri and R. B. Pipes, J. Rheol., 33(7), 1 (1989).
(18) G. K. Batchelor, J. Fluid Mech., 46, 813 (1971).
(19) S. Subbiah, D. L. Trafford and S. I. Guceri; Non-isothermal flow of polymers into two dimensional, thin cavity molds: a numerical grid generation approach; Int. J. Heat Mass Transfer, 32(3), 415 (1989).
(20) C. A. Hieber; Melt viscosity characterisation and its application to injection molding. In A. I. Isayev, editor, Injection and Compression Molding Fundamentals, Marcel Dekker Inc. New York, 1987.